Learning and Nonlinear Models - Journal of the Brazilian Society on Artificial Intelligence (SBIA), Vol. 24, Iss. 2, pp. 4–17, 2026
https://doi.org/10.21528/lnlm-vol24-no2-art1 © Brazilian Society on Artificial Intelligence

# SYSTEMATIC EVALUATION OF FEATURE EXTRACTION AND SELECTION METHODS FOR NOISE-ROBUST EMG-BASED HAND MOVEMENT CLASSIFICATION

**Rafael Ávila dos Santos, Eric F. Schmiele, Leomar Santos Marques, Ricardo Rodrigues Magalhães, Danton Diego Ferreira, Bruno H. G. Barbosa**
Federal University of Lavras
{rafael.santos0t5, eric.robotic}@gmail.com, {leomarmarques, ricardorm, danton, brunohb}@ufla.br

**Resumo –** Os sinais de eletromiograma (EMG) têm sido amplamente utilizados para o controle dos movimentos de próteses robóticas. Nesse contexto, a extração e a seleção de características desempenham papel fundamental na classificação desses sinais em diferentes tipos de movimentos desejados. Embora características no domínio do tempo, como valor absoluto médio, cruzamentos por zero, mudanças de sinal da inclinação, comprimento de forma de onda e entropia amostral, sejam amplamente utilizadas, sua capacidade discriminativa pode ser limitada em condições ruidosas. Este estudo avalia características extraídas por estatísticas de ordem superior (HOS), transformada wavelet discreta (DWT), decomposição wavelet packet (WPD) e características de domínio temporal (TD) para classificação de movimentos a partir de sinais EMG. Adicionalmente, são comparadas quatro técnicas de seleção de características: informação mútua, ReliefF, mRMR e Boruta. Os experimentos foram conduzidos com classificadores MLP, KNN, SVM e RF, considerando sinais originais e sinais com ruído gaussiano em diferentes níveis de SNR. Os resultados indicam que as características baseadas em cumulantes apresentam alta robustez em cenários ruidosos e que a seleção das 25 características mais relevantes pode reduzir substancialmente a dimensionalidade, mantendo ou melhorando o desempenho de classificação.

**Palavras-chave –** Eletromiograma, Prótese Robótica, Cumulantes, Seleção de Características, Transformada Wavelet, Estatística de Ordem Superior.

**Abstract –** Electromyogram (EMG) signals have been extensively utilized for the control of robotic prosthesis movements. In this context, feature extraction and feature selection play a pivotal role in classifying EMG signals into different intended movements. Although time-domain descriptors, such as mean absolute value, zero crossing, slope sign change, waveform length, and sample entropy, are widely used, their discriminative capacity may be limited under noisy conditions. This study evaluates features extracted from higher-order statistics (HOS), discrete wavelet transform (DWT), wavelet packet decomposition (WPD), and time-domain (TD) descriptors for EMG-based movement classification. In addition, four feature selection techniques are compared: mutual information, ReliefF, mRMR, and Boruta. The experiments were conducted using MLP, KNN, SVM, and RF classifiers, considering both original signals and signals corrupted with Gaussian noise at different SNR levels. The results indicate that cumulant-based features are highly robust in noisy scenarios and that selecting the 25 most relevant features can substantially reduce dimensionality while preserving or improving classification performance.

**Keywords –** Electromyogram, Robotic Prosthesis, Cumulants, Feature Selection, Wavelet Transform, Higher-Order Statistics.

## 1. INTRODUCTION

Electromyography (EMG) is the process of measuring the electrical activity of muscles and muscle groups in the human body [1, 2]. As these electric fields are formed by potential actions in different muscle membranes, their waveform properties (frequency, amplitude, etc.) are related to the properties of these membranes [3]. Consequently, it is feasible to extract valuable information from these signals to ascertain the nature of the movement (along with its magnitude and velocity). Consequently, EMG has been extensively utilized in the classification of movements for robotic prostheses [4].

Electromyograms can be acquired in two ways: either by using electrodes placed on the surface of the skin of a subject (surface EMG) or by means of internal electrodes (internal EMG). While internal EMG generates signals with less noise from a specific body part, this method is not usually explored for prosthesis movement since it is invasive. Nevertheless, some researchers have explored the possibility of using internal EMG for prosthesis movement, but the results show no significant difference in the performances [5]. Conversely, surface EMG is predominantly employed for prosthesis movement. However, it is highly susceptible to noise due to the movement of the electrodes, variations in skin composition and thickness, differences in the signals caused by the differential positioning of electrodes, and interference from other biological signals [6].

Furthermore, EMG signals are characterized by an absence of a well-defined waveform, given that they are the result of the sum of the potential action signals from several muscle membranes. Consequently, the extraction of specific features from the signal is necessary for its comprehensive analysis. A plethora of features have been identified for EMG analysis, including the root mean square (RMS) value [2, 7], wavelet packet transform [8], sub-band independent component analysis (SDICA) [6], sample entropy [9], and skewness and kurtosis [10]. However, the most frequently employed features are the mean absolute value (MAV), zero crossing (ZC), slope sign change (SSC), and waveform length (WL), which are closely related to the time-domain

https://doi.org/10.21528/lnlm-vol24-no2-art1 © Brazilian Society on Artificial Intelligence

feature set introduced in early multifunction myoelectric control studies [11–14]. Nevertheless, many studies have attempted to use new features for movement classification, especially because feature quality is one of the central factors affecting EMG pattern-recognition performance [15, 16].

These features are then utilized in the movement classification algorithms. It is notable that the classification algorithms demonstrate significant variation among studies, with the most prevalent algorithms including multilayer perceptron neural networks (MLP), k-nearest neighbors (KNN), support vector machines (SVM), and fuzzy logic [17, 18]. It is important to note that a multitude of other algorithms have been considered. Nevertheless, due to the necessity for prosthesis movement to occur with expediency, the employment of faster classification algorithms is preferable. This requirement is aligned with the standard EMG pattern-recognition pipeline, which typically comprises preprocessing, windowing, feature extraction, dimensionality reduction or feature selection, and classification [15, 19, 20].

Within this broad literature, different feature families have been explored to represent complementary properties of the EMG signal. Time-domain descriptors are computationally simple and remain widely used in real-time myoelectric control. However, several studies have reported redundancy among conventional EMG features and have shown that feature reduction or selection can preserve classification performance while decreasing dimensionality [16, 21]. Time-frequency representations, such as the discrete wavelet transform (DWT) and wavelet packet decomposition (WPD), are also relevant because EMG signals are nonstationary and the discriminative information may vary simultaneously in time and frequency [22]. In addition, public and benchmark-oriented datasets such as Ninapro have reinforced the importance of reproducible comparisons among feature extraction and classification pipelines [23].

Higher-order statistics (HOS) constitute another relevant line of investigation. HOS are defined in terms of moments and cumulants, and their associated Fourier transforms are known as polyspectra [24]. In addition to their efficacy in handling Gaussian measurement noise and extracting information due to deviations from gaussianity, cumulant-based features are not dependent on moments of lower order. From a computational perspective, they are also simpler than polyspectrum-based features [25]. In EMG analysis, Nazarpour et al. proposed surface EMG classification using a selective mix of HOS features [26] and later consolidated the use of HOS for surface electromyogram classification [27]. Orosco et al. also investigated high-order cumulants and bispectrum-based features for muscular-activity detection [28]. These studies indicate that HOS can capture non-Gaussian and nonlinear properties of EMG signals, but they also motivate further investigation of how cumulant orders compare with conventional and wavelet-based descriptors under controlled noise conditions.

Therefore, the present work is positioned at the intersection of three established research directions in EMG pattern recognition: multi-domain feature extraction, robustness analysis, and feature selection. Rather than proposing HOS as a completely unexplored feature family, this study extends previous HOS-based EMG research by jointly evaluating second-, third-, and fourth-order cumulants, conventional time-domain descriptors, DWT, and WPD features under original and noisy signal conditions. In addition, the HOS + TD representation is submitted to four feature selection techniques—mutual information, ReliefF, mRMR, and Boruta—so that compact subsets can be compared not only in terms of classification accuracy, but also according to the type of information retained by each method. This interpretability-oriented analysis is particularly relevant for prosthesis control because a compact feature set can reduce computational cost while preserving discriminative information.

The objectives of this study are twofold. First, the robustness of cumulant-based HOS, TD, DWT, WPD, and combined wavelet-based features is evaluated under additive Gaussian noise by considering different signal-to-noise ratio (SNR) levels. Second, the classification performance obtained with different feature selection techniques is analyzed in order to identify compact and discriminative feature subsets for EMG movement classification, with special attention to the distribution of selected features among second-, third-, and fourth-order cumulants and time-domain descriptors. The scripts used for this work are available in the following repositories: `https://github.com/RafaelGAT108/emg_hos` and `http://www.aia.ufla.br/home/filesdatasets/`.

The remainder of the article is organized as follows: Section 2 presents the methodology adopted for multi-domain feature extraction, noise robustness analysis, feature selection, and classification. In Section 3, the results obtained in a real EMG dataset are presented and discussed. Finally, conclusions and future work are drawn in Section 4.

## 2. METHODOLOGY

The methodology adopted in this work is illustrated in Fig. 1. The experimental protocol was organized into two complementary stages. In the first stage, the objective was to evaluate the discriminative capacity and robustness of different feature families extracted from EMG signals. For this purpose, four groups of features were considered: higher-order statistics (HOS), composed of second-, third-, and fourth-order cumulants; time-domain (TD) features, including MAV, ZC, SSC, WL, and SampEn; discrete wavelet transform (DWT) features; and wavelet packet decomposition (WPD) features.

To assess the robustness of each feature group under noisy conditions, additive Gaussian noise was applied to the original EMG signals considering three signal-to-noise ratio (SNR) levels: 30 dB, 20 dB, and 10 dB. The clean signal condition was also evaluated as a baseline. For each signal condition, the corresponding feature sets were extracted and used as input to a multilayer perceptron (MLP) classifier. The experiments were repeated over 10 independent runs, and the results were reported in terms of mean accuracy and standard deviation for each subject, feature group, and noise level. This stage allows one to quantify how each feature extraction strategy is affected by increasing noise levels and to identify which feature families provide more stable classification performance.

In the second stage, the analysis focused on feature selection and classifier comparison. In this case, the feature pool was

https://doi.org/10.21528/lnlm-vol24-no2-art1 © Brazilian Society on Artificial Intelligence

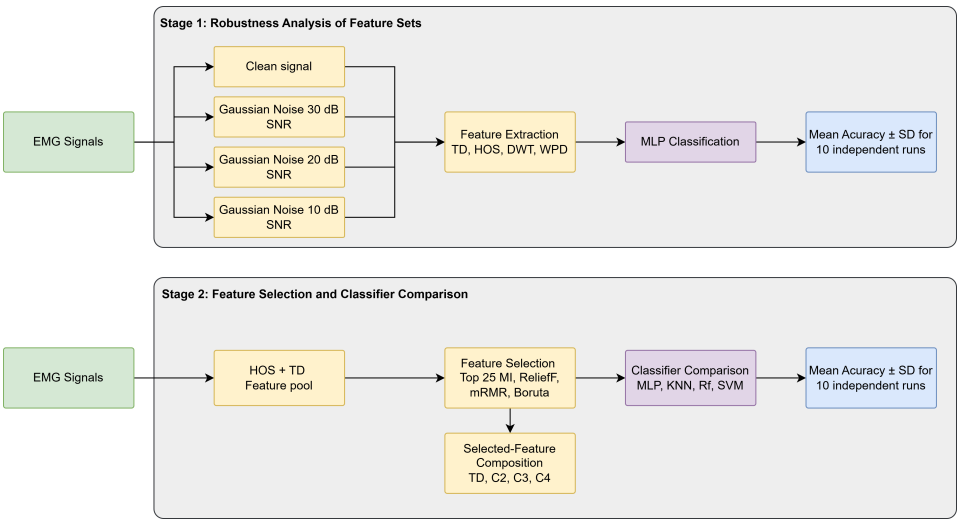



Figure 1: Methodology steps for movements classification.

composed of HOS and TD features, since this combination allows a direct comparison between conventional time-domain descriptors and cumulant-based descriptors. Four feature selection methods were investigated: mutual information (MI), ReliefF, minimum redundancy maximum relevance (mRMR), and Boruta. For each method, the 25 highest-ranked features were selected and subsequently evaluated using four machine learning classifiers: MLP, k-nearest neighbors (KNN), random forest (RF), and support vector machine (SVM).

This second stage evaluates whether the classification performance can be preserved when using a reduced subset of features, while also comparing the behavior of different feature selection methods across classifiers. In addition to classification accuracy, the composition of the selected subsets was analyzed by counting how many of the 25 selected features belonged to each feature category, namely TD features and second-, third-, and fourth-order cumulants. This analysis provides an interpretative perspective on the feature selection process, indicating which types of descriptors are more frequently retained by each selection method.

Finally, statistical analysis and confusion matrices were used as complementary tools to support the interpretation of the classification results. The statistical analysis was employed to assess whether performance differences among methods were significant, while the confusion matrices provided a class-wise view of the recognition performance and the most frequent misclassification patterns.

### 2.1 EMG Dataset

The database was generated by [29] for the classification of basic hand movements using EMG signals. The EMG readings were taken using two surface electrodes on the *flexor carpi ulnaris* and *extensor carpi radialis longus* muscles, sampled with a frequency of 500 Hz and a bandpass filter restricting the range of frequencies from 15 to 500 Hz. In addition, a notch filter set at 50 Hz was used to eliminate power line interference.

The signals were extracted from five healthy volunteers (three women and two men aged between 20 and 22 years) who performed six types of movement thirty times per movement [29]. The movements were classified as cylindrical (C), hook (H), lateral (L), palmar (P), spherical (S), and tip (T). It was not necessary to verify whether a movement occurred, which is generally performed using a mean absolute value of the analysis [30], since the database signals include only movement readings.

The classification and prosthesis movement must be carried out within 300 ms; otherwise, the user will notice a delay in movement and consider the performance of the prosthesis unsatisfactory [31]. Thus, a moving observation window with an extension of 250 ms (an array with 125 observation points considering the sample frequency) and a step of 150 ms was considered, as in [32]. Therefore, the first 100 ms from the second window correspond to the last 100 ms from the first window, and so on, as shown in Fig. 2. Since the duration of each signal was 6 s, a total of 39 windows were acquired from each movement.

In total, there are 39 windows for each signal, resulting in 1170 windows for all movements from the same class and subject. Therefore, there are 7020 windows for each subject.

### 2.2 EMG Feature Extraction

The parameters chosen for this study were the second-, third- and fourth-order cumulants. These were extracted from the signal using HOS, which is considered adequate for non-Gaussian processes and nonlinear systems [33] and has previously shown potential for surface EMG classification and muscular-activity detection [26–28].

https://doi.org/10.21528/lnlm-vol24-no2-art1 © Brazilian Society on Artificial Intelligence

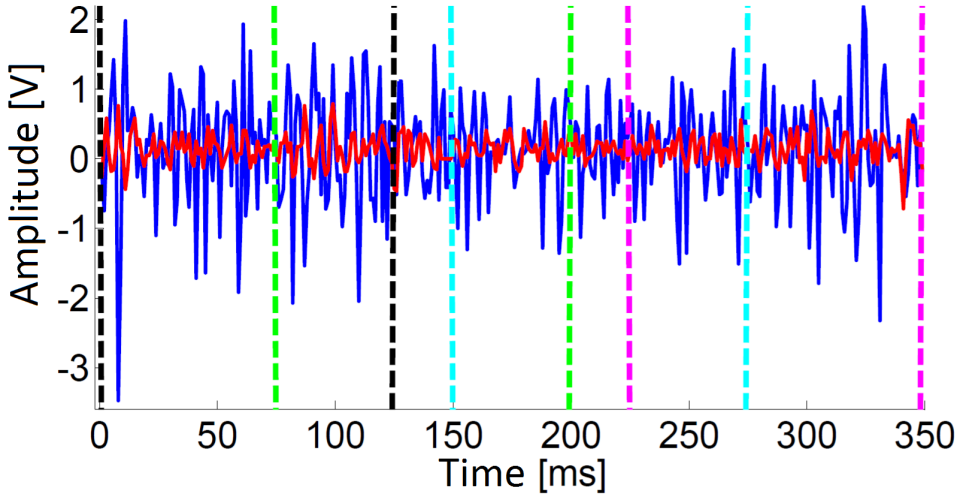



Figure 2: Data windows (Blue: channel 1 from the EMG signal; Red: channel 2 from the EMG signal; Black: Window 1; Green: Window 2; Cyan: Window 3; Magenta: Window 4).

### 2.2.1 Cumulants

According to [33], in a random process $x(t)$ with a group of random variables $(x_1, x_2, ..., x_n)$, for real random variables with zero mean, the second-, third- and fourth-order cumulants are expressed by

$$
\begin{aligned}
cumu(x_1, x_2) &= E(x_1 x_2), && (1)\\
cumu(x_1, x_2, x_3) &= E(x_1 x_2 x_3), && (2)\\
cumu(x_1, x_2, x_3, x_4) &= E(x_1 x_2 x_3 x_4) && (3)\\
&\quad - E(x_1 x_2)E(x_3 x_4)\\
&\quad - E(x_1 x_3)E(x_2 x_4)\\
&\quad - E(x_1 x_4)E(x_2 x_3),
\end{aligned}
$$

where $E$ represents the mathematical expectation operator.

Considering $x(t)$ as a random stationary process with zero mean and the $k$-order cumulants, denoted by $C_{k,x}(\tau_1, \tau_2, ..., \tau_k)$, where $\tau_1$,..., $\tau_k$ are time lags, the second-, third- and fourth-order cumulants can be expressed as, respectively,

$$
\begin{aligned}
C_{2,x}(\tau) &= E\{x(t)x(t+\tau)\},\\
C_{3,x}(\tau) &= E\{x(t)x^2(t+\tau)\}, && (4)\\
C_{4,x}(\tau) &= E\{x(t)x^3(t+\tau)\} - 3C_{2,x}(\tau)C_{2,x}(0).
\end{aligned}
$$

For a discrete signal $x[n]$, equation 4 can be approximated using a circular form to calculate the cumulants, as proposed in [34]:

$$
\begin{aligned}
C_{2,x}(\tau) &= \frac{1}{N}\Sigma_{n=0}^{N-1} x[n]x[mod(n+\tau, N)],\\
C_{3,x}(\tau) &= \frac{1}{N}\Sigma_{n=0}^{N-1} x[n]x^2[mod(n+\tau, N)],\\
C_{4,x}(\tau) &= \frac{1}{N}\Sigma_{n=0}^{N-1} x[n]x^3[mod(n+\tau, N)] && (5)\\
&\quad - 3\frac{1}{N}\Sigma_{n=0}^{N-1} x[n]x[mod(n+\tau, N)].\Sigma_{n=0}^{N-1} x^2[n],
\end{aligned}
$$

where $x \in \Re^N$ and $\tau = 0, 1, ..., N-1$.

### 2.2.2 Time Domain features

In addition to the cumulants, the mean absolute value (MAV), zero crossing (ZC), slope sign change (SSC), waveform length (WL), and sample entropy (SampEn) were also extracted for comparison purposes and to evaluate their combination with the cumulants. These features were obtained by the following equations:

https://doi.org/10.21528/lnlm-vol24-no2-art1 © Brazilian Society on Artificial Intelligence

$$MAV = \frac{1}{N}\sum_{n=1}^{N}\|x_k\|, \tag{6}$$

$$ZC = \begin{cases} 1 & \text{if } (x_k > 0 \,\&\, x_{k+1} < 0) \\ & \text{or } (x_k < 0 \,\&\, x_{k+1} > 0) \\ & k = 1, 2, ..., N-1 \\ 0 & \text{otherwise} \end{cases}, \tag{7}$$

$$SSC = \begin{cases} 1 & \text{if } (x_k < x_{k+1} \,\&\, x_k < x_{k+1}) \\ & \text{or } (x_k > x_{k+1} \,\&\, x_k > x_{k+1}) \\ & k = 1, 2, ..., N-1 \\ 0 & \text{otherwise} \end{cases}, \tag{8}$$

$$WL = \frac{1}{N}\sum_{n=1}^{N-1}\|x_{k+1} - x_k\|, \tag{9}$$

$$SampEn = -\ln\left(\frac{C(m+1,r)}{C(m,r)}\right), \tag{10}$$

where $x$ is the data from a signal, $N$ is the total number of samples from the EMG signal, $m$ is the embedding dimension and defined as 2, $r$ is the tolerance equal to $0.2 \times$ std$(x)$, $C(m+1,r)$ is the number of embedded vectors of length $m+1$ having a Chebyshev distance inferior to $r$, and $C(m,r)$ is the number of embedded vectors of length $m$ having a Chebyshev distance of less than $r$.

After the feature extraction step, the time-domain features were organized into an array containing MAV, ZC, SSC, WL, and SampEn for each EMG channel. The cumulant-based HOS array contained 624 elements, including second-, third-, and fourth-order cumulants computed for both EMG channels. These descriptors were evaluated individually and in combination with the wavelet-based feature sets described next.

### 2.2.3 Discrete Wavelet Transform

The discrete wavelet transform (DWT) decomposes a signal into approximation and detail components using a pair of low-pass and high-pass filters followed by downsampling. For an input signal $x[n]$, the approximation and detail coefficients at decomposition level $j$ can be represented as

$$A_j[k] = \sum_n h[n-2k]A_{j-1}[n], \tag{11}$$

$$D_j[k] = \sum_n g[n-2k]A_{j-1}[n], \tag{12}$$

where $A_{j-1}[n]$ is the approximation signal from the previous level, $h[\cdot]$ and $g[\cdot]$ are the low-pass and high-pass analysis filters, respectively, and $A_0[n] = x[n]$. In this work, the DWT coefficients were used to represent the EMG signal in a time-frequency domain, allowing transient and nonstationary components associated with muscle activation to be considered in the classification process.

### 2.2.4 Wavelet Packet Decomposition

Wavelet packet decomposition (WPD) extends the DWT by decomposing both approximation and detail components at each level. Consequently, WPD provides a more detailed partition of the time-frequency plane than the standard DWT, which may be useful for EMG signals because relevant movement information can be distributed across different frequency subbands. Let $W_j^p[k]$ denote the coefficients of node $p$ at level $j$. The next-level nodes can be obtained as

$$W_{j+1}^{2p}[k] = \sum_n h[n-2k]W_j^p[n], \tag{13}$$

$$W_{j+1}^{2p+1}[k] = \sum_n g[n-2k]W_j^p[n], \tag{14}$$

where $W_0^0[n] = x[n]$. The WPD-based feature vector was constructed from the coefficients obtained from the decomposition tree and evaluated as an alternative representation to HOS, TD, and DWT features.

https://doi.org/10.21528/lnlm-vol24-no2-art1 © Brazilian Society on Artificial Intelligence

### 2.3 Signal-to-Noise Ratio

Signal-to-noise ratio (SNR) measures the relative level between the useful signal and the noise component, usually expressed in decibels (dB). In this work, SNR is used to generate controlled noisy versions of the original EMG signals and to evaluate the robustness of the extracted features. Lower SNR values indicate stronger noise contamination; therefore, 10 dB represents a more challenging condition than 20 dB and 30 dB. Considering an original signal $x[n]$ and additive noise $v[n]$, the SNR can be expressed as

$$SNR_{dB} = 10 \log_{10} \left( \frac{P_x}{P_v} \right), \tag{15}$$

where $P_x$ and $P_v$ are the signal and noise powers, respectively.

### 2.4 Feature Selection

The feature selection step is important to reduce data dimensionality, which may improve classification accuracy, reduce model complexity, and decrease computational cost. This is particularly relevant in EMG-based prosthesis control, where fast and reliable decisions are required. Previous EMG studies have shown that many extracted descriptors can be redundant and that reduced subsets may be sufficient for accurate classification [16,21]. In this work, four feature selection techniques are compared: mutual information (MI) [35], ReliefF [36], minimum redundancy maximum relevance (mRMR) [37], and Boruta [38]. For a fair comparison among the methods, the 25 most relevant features selected or ranked by each technique were used as classifier inputs.

#### 2.4.1 Mutual Information

Mutual Information (MI) measures the statistical dependence between two random variables. In feature selection, it is commonly used to quantify how much information a feature provides about the class label. The mutual information between a feature $X$ and a class variable $Y$ is defined as

$$I(X;Y) = \sum_{x \in X} \sum_{y \in Y} p(x,y) \log \left( \frac{p(x,y)}{p(x)p(y)} \right), \tag{16}$$

where $p(x,y)$ is the joint probability distribution and $p(x)$ and $p(y)$ are the marginal probability distributions. In the feature selection context, the relevance of a feature $f_i$ with respect to the class label $C$ can be written as

$$MI(f_i, C) = \sum_{f_i} \sum_{C} p(f_i, C) \log \left( \frac{p(f_i, C)}{p(f_i)p(C)} \right). \tag{17}$$

Features with higher $MI(f_i, C)$ values are considered more relevant because they reduce the uncertainty about the class labels. In this work, the MI criterion was used to rank the features, and the top 25 features were selected for classifier training.

#### 2.4.2 ReliefF

ReliefF assigns a weight to each feature according to its ability to distinguish neighboring samples from different classes while preserving similarity among samples from the same class. For each randomly selected instance $R$, the algorithm finds its $k$ nearest neighbors from the same class, called nearest hits $H_j$, and its $k$ nearest neighbors from each different class, called nearest misses $M_j(C)$. The weight update for an attribute $A$ is given by

$$W[A] = W[A] - \frac{1}{m} \sum_{j=1}^{k} \text{diff}(A, R, H_j) + \frac{1}{m} \sum_{C \neq class(R)} \frac{P(C)}{1 - P(class(R))} \sum_{j=1}^{k} \text{diff}(A, R, M_j(C)), \tag{18}$$

where $m$ is the number of sampled instances, $P(C)$ is the prior probability of class $C$, and $class(R)$ is the class of instance $R$. The function $\text{diff}(\cdot)$ measures the normalized distance between two samples for a given feature:

$$\text{diff}(A, x_1, x_2) = \frac{|x_1(A) - x_2(A)|}{\max(A) - \min(A)}. \tag{19}$$

Thus, features receive higher weights when they present small differences between samples of the same class and large differences between samples of different classes. The 25 features with the highest ReliefF weights were selected.

https://doi.org/10.21528/lnlm-vol24-no2-art1 © Brazilian Society on Artificial Intelligence

### 2.4.3 Minimum Redundancy Maximum Relevance

mRMR (minimum redundancy maximum relevance) is a feature selection technique that searches for a subset of features that is simultaneously relevant to the class labels and minimally redundant within the selected subset. Unlike univariate ranking methods, mRMR considers the relationship among candidate features in addition to their individual relationship with the target class. Let $S$ be the selected feature subset and $c$ the class label. The maximum relevance term is defined as

$$D = \frac{1}{|S|} \sum_{x_i \in S} I(x_i; c), \tag{20}$$

while the redundancy term is defined as

$$R = \frac{1}{|S|^2} \sum_{x_i, x_j \in S} I(x_i; x_j). \tag{21}$$

The mRMR criterion can then be written as

$$\Phi(D, R) = D - R, \tag{22}$$

where high values of $D$ indicate strong dependence between the selected features and the class labels, whereas low values of $R$ indicate low redundancy among the selected features. In this work, the mRMR criterion was used to select the 25 features that best balanced relevance and redundancy.

### 2.4.4 Boruta

Boruta is a wrapper feature selection technique based on Random Forest importance scores. The method creates shadow features by randomly permuting the original attributes, trains a Random Forest model using the original and shadow features, and compares the importance of each original feature with the best shadow feature. The main acceptance rule can be expressed as

$$Z_i > \max(Z_{\text{shadow}}), \tag{23}$$

where $Z_i$ is the importance score of the original feature $i$ and $\max(Z_{\text{shadow}})$ is the maximum importance score among the shadow features. Features that consistently achieve higher importance than the shadow attributes are considered relevant, whereas features with lower importance are rejected. In this work, Boruta was used to rank the relevant attributes, and the top 25 features were retained for the classification stage.

## 2.5 Classification Algorithms

The feature vectors were obtained by segmenting the original signals into the analysis windows shown in Fig. 2. Each subject was evaluated independently, since EMG signals vary considerably across individuals and may also be affected by electrode placement [6].

In this study, KNN, RF, MLO and SVM classifiers were implemented and evaluated under the feature configurations described in the previous sections.

### 2.5.1 k-Nearest Neighbor (KNN)

The KNN algorithm is a simple and widely used machine learning classifier. Its training procedure consists of storing the labeled samples from the training set. To classify a new input, the algorithm searches for the $k$ closest known samples according to a distance metric. The final class is then assigned by a voting process among the nearest neighbors.

Two factors strongly affect KNN performance: the number of neighbors and the distance metric. The value of $k$ determines how many neighboring samples are considered when assigning the class of a new data point.

Another factor that can reduce the performance of the method is the dimensionality of the input pattern. When dimensionality increases, distances become less informative and computational cost increases; therefore, feature selection is used to obtain a compact and more discriminative input representation.

### 2.5.2 Random Forest (RF)

Random Forest (RF) is a classifier based on an ensemble of decision trees. This ensemble strategy can improve accuracy and reduce overfitting by combining multiple trees trained with random subsets of samples and features. Thus, each tree contributes an individual prediction based on a different view of the input data.

The final RF prediction is obtained by majority voting among the internal decision trees.

https://doi.org/10.21528/lnlm-vol24-no2-art1 © Brazilian Society on Artificial Intelligence

#### 2.5.3 Multilayer Perceptron (MLP) Neural Network

The MLP is a feedforward neural network classifier composed of an input layer, one or more hidden layers, and an output layer. The input layer receives the feature vector, the hidden layer performs nonlinear transformations, and the output layer provides the class probabilities. Because the MLP can model nonlinear decision boundaries and its topology can be adapted to the problem, it is a flexible classifier for EMG movement recognition.

There are several algorithms to estimate the parameters of an MLP network. In this paper, the Nadam optimizer was used. The hyperbolic tangent activation function was adopted in the hidden neurons, and the softmax function was used in the output neurons.

The size of the MLP input layer was adjusted according to the evaluated feature configuration. Thus, when all features were used, the input layer contained the complete feature vector, whereas in the feature selection experiments the input layer contained the 25 selected features. The final MLP topology has 10 neurons in the hidden layer and 6 neurons in the output layer.

#### 2.5.4 Support Vector Machine (SVM)

The SVM algorithm defines a decision hyperplane that separates the data classes. The optimization criterion seeks the hyperplane with the largest margin with respect to the closest training samples, which are called support vectors. Kernel functions can also be used to increase the flexibility of the method and enable the classification of nonlinearly separable data.

The advantages of the SVM algorithm include robustness against overfitting and the ability to deal with high-dimensional data. Another important aspect is that SVM can achieve satisfactory performance even when the number of samples is limited compared with the dimensionality of the input data [39].

### 2.6 Validation

The classification accuracy was adopted as the main performance metric. It represents the percentage of correctly classified EMG windows in the validation set. Since a single train-test split may favor a particular data partition, a stratified validation procedure was adopted to preserve the proportion of the six movement classes in each fold.

In this work, the dataset of each subject was evaluated independently using stratified 3-fold cross-validation. In each fold, approximately 66.6% of the samples were used for training and 33.3% for validation. The procedure was repeated over 10 independent runs in order to account for randomness in the classifiers and in the data partitioning process. The reported values correspond to the mean accuracy and standard deviation across these runs.

For the feature selection experiments, the selection procedure was applied to the HOS + TD feature set and the 25 selected features were used to train the classifiers. This protocol enables a direct comparison among MI, ReliefF, mRMR, and Boruta in terms of classification accuracy, variance, and selected feature categories.

## 3. RESULTS AND DISCUSSION

### 3.1 HOS-features Analysis

Fig. 3 illustrates the mean values for Woman 1 of the second-, third-, and fourth-order cumulants extracted from cylindrical (C), hook (H), lateral (L), palmar (P), spherical (S), and tip (T) movements. It can be inferred that each class presents a different signature pattern according to its cumulants, indicating that HOS is a promising feature extraction tool for EMG-based prosthesis control. Fig. 3 also shows that cumulant-based representations provide a more structured description of the signal when compared with the raw EMG waveform.

The raw EMG signals present high variability across windows and movements, which can make the classification task difficult. However, the cumulant representations reveal visually distinguishable movement patterns. The supplementary material shows the cumulants extracted from the other subjects signals.

### 3.2 Classification of EMG signals

Table 1 presents the classification results obtained for the different subjects and signal conditions using the evaluated feature extraction domains: HOS, TD, HOS + TD, DWT, WPD, and DWT + WPD. In this first analysis, only the MLP classifier is reported because the objective is to compare the discriminative capacity and noise robustness of the feature representations without dimensionality reduction. Therefore, all extracted features from each configuration were used as classifier inputs.

The results show that HOS features achieved the highest or among the highest accuracies for all subjects and noise conditions, with low standard deviations. This behavior indicates that cumulant-based descriptors are robust to additive Gaussian noise and provide discriminative information for EMG movement classification. The TD features presented substantially lower performance and higher variability, especially under more severe noise conditions, which reinforces the limitation of using only conventional time-domain descriptors. The DWT and WPD representations also achieved competitive results, particularly when compared with TD features, showing that wavelet-based time-frequency information is useful for this task.

Statistical analysis was also performed using the Nemenyi post-hoc test. In this technique, p-values lower than 0.05 indicate statistically significant differences between feature configurations. As shown in Fig. 4, the post-hoc analysis complements

https://doi.org/10.21528/lnlm-vol24-no2-art1 © Brazilian Society on Artificial Intelligence

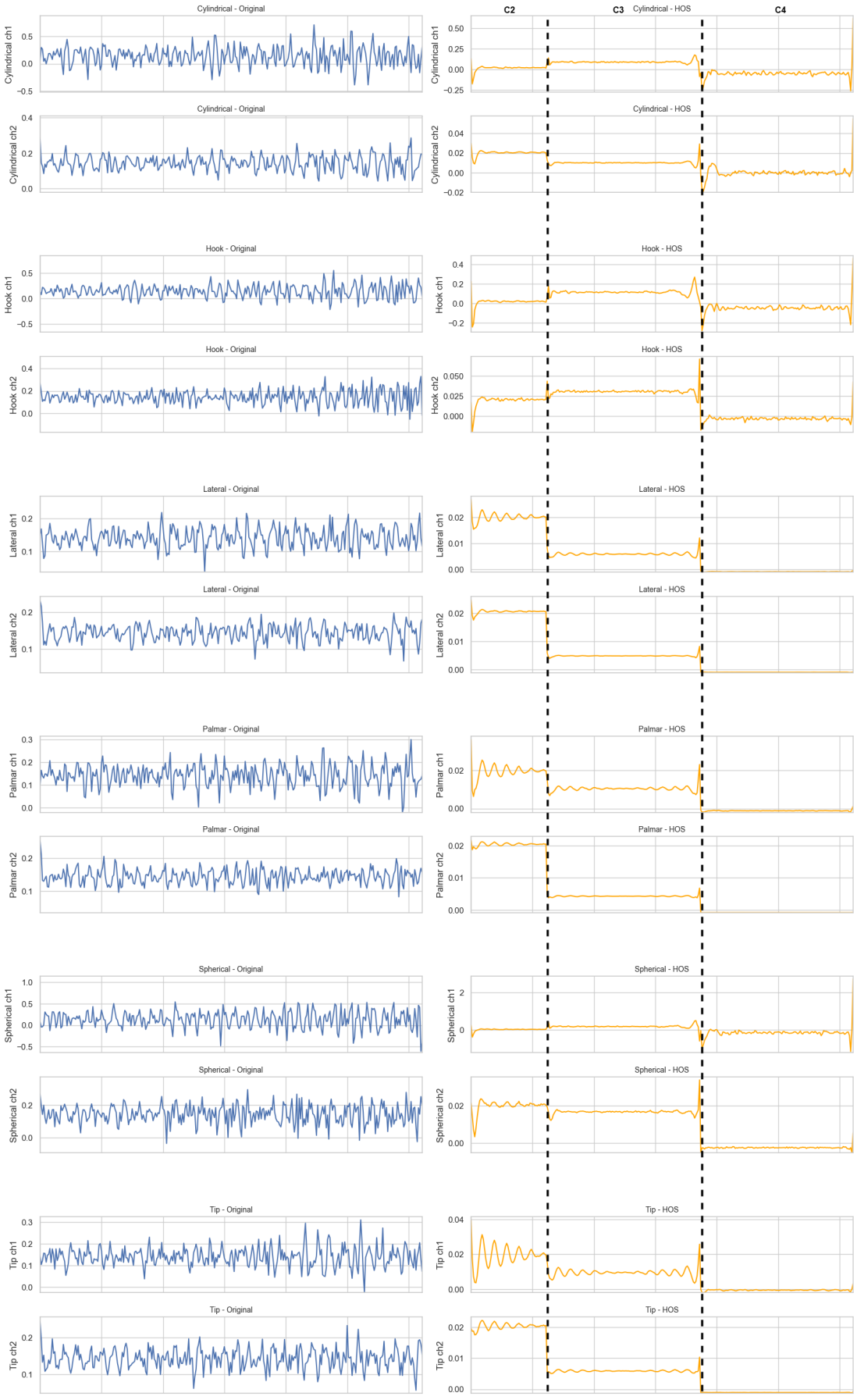



Figure 3: Comparison between the original EMG signal and the signal cumulants of 2nd (C2), 3rd (C3) and 4th (C4) orders.

https://doi.org/10.21528/lnlm-vol24-no2-art1 © Brazilian Society on Artificial Intelligence

Table 1: Mean validation accuracy (%) and standard deviation over 10 runs for each subject, signal condition, and feature set.

| Subject | Condition | Validation (%) | | | | | |
|---|---|---|---|---|---|---|---|
| | | HOS | TD | HOS + TD | DWT | WPD | DWT + WPD |
| man 1 | Default | 98.84 ± 0.24 | 75.55 ± 11.91 | 83.66 ± 1.20 | 97.43 ± 0.74 | 97.11 ± 0.36 | 87.65 ± 0.82 |
| | Noise 30dB | 98.72 ± 0.33 | 75.87 ± 6.87 | 82.88 ± 2.35 | 97.36 ± 0.99 | 96.78 ± 0.40 | 87.08 ± 0.85 |
| | Noise 20dB | 98.83 ± 0.19 | 77.27 ± 7.35 | 83.89 ± 0.68 | 97.73 ± 0.66 | 97.06 ± 0.34 | 86.56 ± 0.74 |
| | Noise 10dB | 98.70 ± 0.39 | 68.12 ± 20.98 | 79.99 ± 1.75 | 97.22 ± 0.50 | 97.09 ± 0.34 | 85.66 ± 0.69 |
| man 2 | Default | 99.17 ± 0.21 | 75.65 ± 16.56 | 93.14 ± 0.77 | 96.75 ± 1.21 | 96.66 ± 0.43 | 91.35 ± 0.55 |
| | Noise 30dB | 98.71 ± 0.36 | 73.47 ± 10.87 | 83.99 ± 1.24 | 95.50 ± 5.15 | 96.94 ± 0.59 | 91.91 ± 0.59 |
| | Noise 20dB | 98.80 ± 0.29 | 72.70 ± 15.54 | 82.67 ± 1.14 | 97.38 ± 1.14 | 96.74 ± 0.61 | 91.68 ± 0.80 |
| | Noise 10dB | 98.64 ± 0.30 | 75.07 ± 6.87 | 81.12 ± 1.15 | 95.97 ± 1.37 | 96.55 ± 0.63 | 91.04 ± 0.62 |
| woman 1 | Default | 96.31 ± 0.29 | 75.78 ± 11.42 | 79.45 ± 1.26 | 94.03 ± 1.01 | 94.00 ± 0.58 | 79.25 ± 0.80 |
| | Noise 30dB | 96.50 ± 0.42 | 74.18 ± 13.72 | 78.76 ± 3.24 | 94.66 ± 1.29 | 94.41 ± 0.58 | 79.47 ± 0.74 |
| | Noise 20dB | 96.27 ± 0.45 | 75.82 ± 12.89 | 79.95 ± 1.07 | 94.58 ± 1.30 | 94.14 ± 0.36 | 79.52 ± 0.87 |
| | Noise 10dB | 96.60 ± 0.38 | 66.75 ± 19.75 | 78.21 ± 1.80 | 93.89 ± 1.80 | 95.34 ± 0.53 | 78.84 ± 1.98 |
| woman 2 | Default | 95.07 ± 0.98 | 58.59 ± 14.07 | 75.34 ± 1.96 | 89.71 ± 2.50 | 88.15 ± 1.72 | 69.06 ± 1.37 |
| | Noise 30dB | 94.24 ± 0.68 | 62.56 ± 12.64 | 75.00 ± 1.88 | 91.28 ± 2.42 | 87.92 ± 1.72 | 69.37 ± 1.32 |
| | Noise 20dB | 95.18 ± 0.66 | 61.37 ± 12.43 | 74.37 ± 1.95 | 91.26 ± 3.12 | 88.01 ± 2.31 | 68.18 ± 1.01 |
| | Noise 10dB | 94.32 ± 0.56 | 68.09 ± 6.72 | 74.46 ± 1.54 | 91.91 ± 3.12 | 87.73 ± 2.44 | 69.53 ± 1.41 |
| woman 3 | Default | 97.25 ± 0.29 | 81.42 ± 11.34 | 76.81 ± 1.17 | 96.79 ± 2.24 | 97.12 ± 0.35 | 83.80 ± 1.13 |
| | Noise 30dB | 97.49 ± 0.32 | 75.87 ± 12.30 | 77.06 ± 1.85 | 96.96 ± 0.62 | 97.24 ± 0.30 | 83.61 ± 1.00 |
| | Noise 20dB | 97.41 ± 0.20 | 78.75 ± 10.48 | 76.31 ± 2.24 | 97.41 ± 0.42 | 97.22 ± 0.43 | 83.10 ± 1.37 |
| | Noise 10dB | 98.29 ± 0.19 | 72.82 ± 10.34 | 75.50 ± 1.38 | 98.02 ± 0.47 | 97.92 ± 0.28 | 83.11 ± 0.82 |

the descriptive results by indicating which feature extraction strategies present statistically distinguishable classification behavior. Overall, these results suggest that HOS and wavelet-based representations are promising alternatives for EMG movement classification, whereas TD features alone may be insufficient for robust classification under noisy conditions.




Figure 4: Results from Post-hoc Nemenyi p-values (highlight for $p < 0.05$)

Although the results obtained with complete feature sets are useful to compare extraction domains, the high dimensionality of HOS + TD features may increase computational cost and introduce redundant information. Therefore, feature selection methods were applied to investigate whether compact subsets could preserve or improve classification performance. The KNN classifier used 10 neighbors, the MLP neural network used a learning rate of 0.001 and 10 neurons in the hidden layer, and the SVM classifier used a linear kernel with penalty parameter $C$ equal to 1.

The feature selection analysis focuses on the HOS + TD representation because it allows the selected features to be interpreted according to their categories: second-order cumulants, third-order cumulants, fourth-order cumulants, and time-domain descriptors. This analysis makes it possible not only to compare classification accuracy, but also to understand which feature families are most frequently retained by each selection technique.

As a matter of practicality, only the confusion matrix of the individual with the best classification performance is shown, which is the case of man 2 under the Random Forest Classifier (see Fig. 5). As can be seen, most of the classes obtained a high classification performance. Most of the errors happened between the classes Hook and Lateral.

https://doi.org/10.21528/lnlm-vol24-no2-art1 © Brazilian Society on Artificial Intelligence

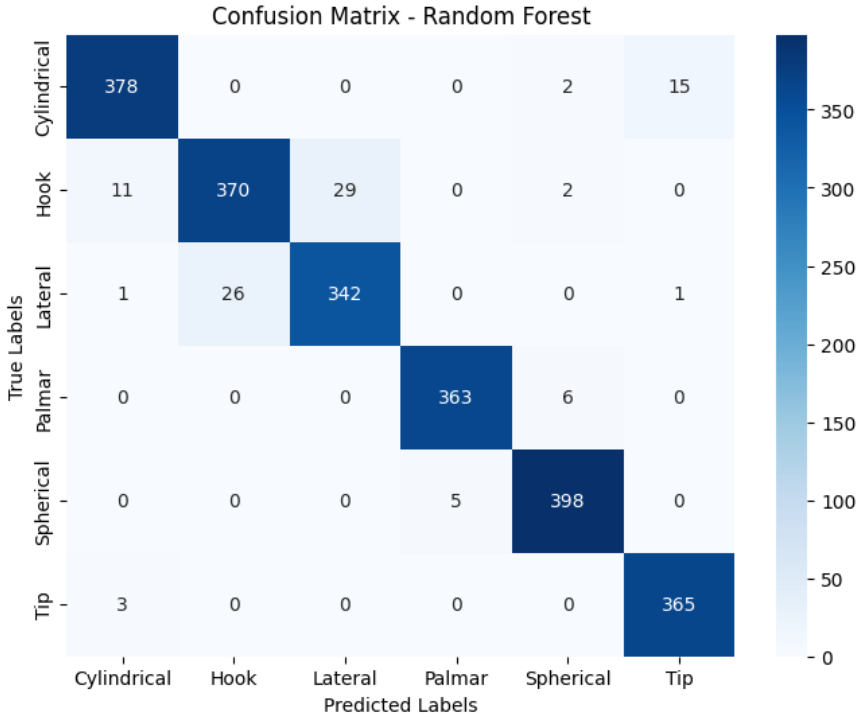



Figure 5: Confusion matrix of the Random Forest for man 2.

### 3.3 Classification with top 25 feature selection of EMG signals

Table 2 presents the mean accuracy and standard deviation over 10 runs for the Female 2 subject using the MLP, KNN, SVM, and RF classifiers. For each classifier, the table compares the use of all HOS + TD features with the top 25 features selected by MI, ReliefF, mRMR, and Boruta. Complementarily, Table 3 reports the corresponding average results considering all five subjects evaluated in this work.

The results indicate that ReliefF and mRMR achieved the most consistent performance among the evaluated feature selection techniques. This result is relevant because the selected subsets reduce the dimensionality from 634 features to only 25 features, corresponding to a reduction of approximately 96%. In several cases, the selected subsets also improved the mean accuracy or reduced the standard deviation when compared with the use of all features, suggesting that the removed features were either redundant or less informative for the classification task.

Among the four machine learning models, Random Forest obtained the best overall performance in most evaluated cases. This result is consistent with the ensemble nature of RF, which combines multiple decision trees and tends to reduce variance when compared with single-model classifiers such as MLP, KNN, and SVM.

To interpret the feature subsets obtained by the selection techniques, Table 4 shows how the 25 selected features are distributed among second-order cumulants (C2), third-order cumulants (C3), fourth-order cumulants (C4), and time-domain features (TD). The best-performing selection methods did not retain fourth-order cumulants, instead selecting a balanced combination of C2, C3, and TD features. In contrast, Boruta selected a high number of fourth-order cumulants and produced lower classification accuracy. This behavior suggests that, for the evaluated dataset and experimental protocol, fourth-order cumulants may provide less discriminative information than second- and third-order cumulants. This interpretation is also supported by Fig. 3, where the segment corresponding to fourth-order cumulants appears less clearly associated with movement-specific patterns.

Table 2: Classification accuracy (%) for the Woman 2 subject under different feature selection methods using HOS + TD and Default signal.

| Feature Selection | MLP | KNN | SVM | RF |
|---|---|---|---|---|
| ALL | $65.09 \pm 2.86$ | $67.45 \pm 1.16$ | $\mathbf{78.22 \pm 0.56}$ | $79.89 \pm 0.87$ |
| MI | $67.11 \pm 1.05$ | $\mathbf{76.85 \pm 0.65}$ | $72.06 \pm 0.75$ | $82.70 \pm 0.78$ |
| ReliefF | $\mathbf{69.49 \pm 1.45}$ | $73.43 \pm 0.81$ | $76.60 \pm 0.51$ | $84.95 \pm 0.75$ |
| mRMR | $68.92 \pm 1.56$ | $73.87 \pm 0.64$ | $75.79 \pm 0.91$ | $\mathbf{84.99 \pm 0.81}$ |
| Boruta | $63.76 \pm 1.38$ | $66.16 \pm 0.85$ | $66.52 \pm 1.44$ | $78.95 \pm 0.98$ |

Table 3: Average classification accuracy (%) across all subjects for different feature selection methods and classifiers.

| Feature Selection | MLP | KNN | SVM | RF |
|---|---|---|---|---|
| ALL | $76.86 \pm 9.12$ | $78.26 \pm 8.16$ | $\mathbf{83.30 \pm 6.35}$ | $87.09 \pm 5.52$ |
| MI | $69.09 \pm 8.08$ | $\mathbf{81.46 \pm 5.52}$ | $75.01 \pm 7.35$ | $84.93 \pm 5.24$ |
| ReliefF | $77.07 \pm 4.72$ | $79.47 \pm 5.48$ | $80.26 \pm 4.26$ | $87.76 \pm 3.84$ |
| mRMR | $\mathbf{78.07 \pm 6.36}$ | $80.49 \pm 6.12$ | $81.27 \pm 5.75$ | $\mathbf{88.36 \pm 4.04}$ |
| Boruta | $57.61 \pm 11.11$ | $76.79 \pm 6.32$ | $66.24 \pm 9.32$ | $82.49 \pm 4.35$ |

Table 4: Distribution of selected features according to their category for each feature selection method.

| Method | C2 | C3 | C4 | TD |
|---|---|---|---|---|
| Boruta | 1 | 0 | 18 | 6 |
| MI | 2 | 18 | 1 | 4 |
| **ReliefF** | 9 | 6 | 0 | 10 |
| **mRMR** | 10 | 8 | 0 | 7 |

## 4. CONCLUSIONS AND FUTURE WORK

This study evaluated multi-domain feature extraction and feature selection techniques for EMG-based hand movement classification. The analysis considered HOS features based on second-, third-, and fourth-order cumulants, conventional time-domain descriptors, and wavelet-based representations obtained from DWT and WPD. The database contained EMG signals from six hand movements, and the experiments were conducted independently for each subject using MLP, KNN, SVM, and RF classifiers.

The results showed that cumulant-based HOS features achieved high classification accuracy and low variability under the evaluated noise conditions, indicating robustness to additive Gaussian noise. Wavelet-based representations also provided competitive performance, whereas TD features alone presented lower accuracy and higher variance. These findings reinforce the importance of using feature representations that capture nonlinear and time-frequency characteristics of EMG signals.

The comparison among MI, ReliefF, mRMR, and Boruta demonstrated that feature selection can substantially reduce dimensionality while preserving or improving classification performance. In particular, ReliefF and mRMR provided the most consistent results, reducing the input space from 634 features to 25 features, approximately a 96% reduction. Random Forest presented the best overall classification performance among the evaluated classifiers. The analysis of the selected feature categories also indicated that second- and third-order cumulants, together with TD descriptors, were more frequently associated with high classification accuracy than fourth-order cumulants.

For future work, feature selection approaches that automatically determine the number of selected features should be investigated, since the methods evaluated in this study require the number of retained features to be specified as a hyperparameter. Multiobjective optimization may also be explored to explicitly model the trade-off between classification accuracy, number of features, and computational cost. In addition, different neural network architectures, ensemble strategies, and subject-independent validation protocols may be evaluated to further assess the robustness and generalization capability of the proposed methodology.

## 5 ACKNOWLEDGMENTS

Authors would like to thank FAPEMIG (*Fundação de Amparo à Pesquisa de Minas Gerais*), FAPESP (*Fundação de Amparo à Pesquisa de São Paulo*) and CNPq (*National Council for Scientific and Technological Development*) for their financial support.

## REFERENCES

[1] A. Saikia, S. Mazumdar, N. Sahai, S. Paul and D. Bhatia. "Performance analysis of artificial neural network for hand movement detection from EMG signals". *IETE Journal of Research*, vol. 68, no. 2, pp. 1074–1083, 2022. doi: 10.1080/03772063.2019.1638316.

[2] S. I. Khan and R. B. Pachori. "Automated Eye Movement Classification Based on EMG of EOM Signals Using FBSE-EWT Technique". *IEEE Transactions on Human-Machine Systems*, vol. 53, no. 2, pp. 346–356, 2023. doi: 10.1109/THMS.2023.3238113.

[3] M. D. Binder, N. Hirokawa and U. Windhorst. *Encyclopedia of neuroscience*. 2009. doi: 10.1007/978-3-540-29678-23043.

[4] P. A. Parker and R. N. Scott. "Myoelectric control of prostheses". *Critical reviews in biomedical engineering*, vol. 13, no. 4, pp. 283–310, 1986. PMID: 3512166.

[5] Y. Fang, N. Hettiarachchi, D. Zhou and H. Liu. "Multimodal sensing techniques for interfacing hand prostheses: a review". *IEEE Sensors Journal*, vol. 15, no. 11, pp. 6065–6076, 2015. doi: 10.1109/JSEN.2015.2450211.

[6] G. R. Naik, K. G. Baker and H. T. Nguyen. "Dependence independence measure for posterior and anterior EMG sensors used in simple and complex finger flexion movements: Evaluation using SDICA". *IEEE journal of biomedical and health informatics*, vol. 19, no. 5, pp. 1689–1696, 2015. doi: 10.1109/JBHI.2014.2340397.

[7] T. Triwiyanto, O. Wahyunggoro, H. A. Nugroho and H. Herianto. "Muscle fatigue compensation of the electromyography signal for elbow joint angle estimation using adaptive feature". *Computers & Electrical Engineering*, vol. 71, pp. 284–293, 2018. doi: 10.1016/j.compeleceng.2018.07.026.

[8] S. Pancholi and A. M. Joshi. "Improved classification scheme using fused wavelet packet transform based features for intelligent myoelectric prostheses". *IEEE Transactions on Industrial Electronics*, 2019. doi: 10.1109/TIE.2019.2946536.

[9] N. Phukan and N. M. Kakoty. "Sample Entropy Based Selection of Wavelet Decomposition Level for Finger Movement Recognition Using EMG". In *Progress in Advanced Computing and Intelligent Engineering*, pp. 61–73. 2019. doi: 10.1007/978-981-13-1708-86.

[10] C. Zhang, X. Chen, S. Cao, X. Zhang and X. Chen. "A novel HD-sEMG preprocessing method integrating muscle activation heterogeneity analysis and kurtosis-guided filtering for high-accuracy joint force estimation". *IEEE Transactions on Neural Systems and Rehabilitation Engineering*, vol. 27, no. 9, pp. 1920–1930, 2019. doi: 10.1109/TNSRE.2019.2933811.

[11] B. Hudgins, P. Parker and R. N. Scott. "A new strategy for multifunction myoelectric control". *IEEE Transactions on Biomedical Engineering*, vol. 40, no. 1, pp. 82–94, 1993.

[12] J. Luo, C. Liu and C. Yang. "Estimation of EMG-based force using a neural-network-based approach". *IEEE Access*, vol. 7, pp. 64856–64865, 2019. doi: 10.1109/ACCESS.2019.2917300.

[13] H. K. Hameed, W. Z. Hasan, S. Shafie, S. A. Ahmad and H. Jaafar. "An amplitude independent muscle activity detection algorithm based on adaptive zero crossing technique and mean instantaneous frequency of the sEMG signal". In *2017 IEEE Regional Symposium on Micro and Nanoelectronics (RSM)*, pp. 183–186, 2017. doi: 10.1109/RSM.2017.8069133.

[14] Y. Paul, V. Goyal and R. A. Jaswal. "Comparative analysis between SVM & KNN classifier for EMG signal classification on elementary time domain features". In *2017 4th International Conference on Signal Processing, Computing and Control (ISPCC)*, pp. 169–175, 2017. doi: 10.1109/ISPCC.2017.8269670.

[15] E. Scheme and K. Englehart. "Electromyogram pattern recognition for control of powered upper-limb prostheses: State of the art and challenges for clinical use". *Journal of Rehabilitation Research and Development*, vol. 48, no. 6, pp. 643–659, 2011.

[16] A. Phinyomark, R. N. Khushaba and E. Scheme. "Feature extraction and selection for myoelectric control based on wearable EMG sensors". *Sensors*, vol. 18, no. 5, pp. 1615, 2018.

[17] C. Guevara, J. Jadán-Guerrero, Y. Rybarczyk, P. Acosta-Vargas, W. Esparza, M. González, S. Villarreal, S. Sanchez-Gordon, T. Calle-Jimenez and I. L. Nunes. "A Real-Time Algorithm for Movement Assessment Using Fuzzy Logic of Hip Arthroplasty Patients". In *International Conference on Applied Human Factors and Ergonomics*, pp. 265–273, 2018. doi: 10.1007/978-3-319-94334-327.

[18] N. Sezgin. "A new hand finger movements' classification system based on bicoherence analysis of two-channel surface EMG signals". *Neural Computing and Applications*, vol. 31, no. 8, pp. 3327–3337, 2019. doi: 10.1007/s00521-017-3286-z.

[19] M. A. Oskoei and H. Hu. "Myoelectric control systems—A survey". *Biomedical Signal Processing and Control*, vol. 2, no. 4, pp. 275–294, 2007.

[20] R. H. Chowdhury, M. B. I. Reaz, M. A. B. M. Ali, A. A. A. Bakar, K. Chellappan and T. G. Chang. "Surface electromyography signal processing and classification techniques". *Sensors*, vol. 13, no. 9, pp. 12431–12466, 2013.

[21] A. Phinyomark, P. Phukpattaranont and C. Limsakul. "Feature reduction and selection for EMG signal classification". *Expert Systems with Applications*, vol. 39, no. 8, pp. 7420–7431, 2012.

[22] K. Englehart and B. Hudgins. "A robust, real-time control scheme for multifunction myoelectric control". *IEEE Transactions on Biomedical Engineering*, vol. 50, no. 7, pp. 848–854, 2003.

[23] M. Atzori, A. Gijsberts, C. Castellini, B. Caputo, A.-G. M. Hager, S. Elsig, G. Giatsidis, F. Bassetto and H. Muller. "Electromyography data for non-invasive naturally-controlled robotic hand prostheses". *Scientific Data*, vol. 1, pp. 140053, 2014.

[24] J. D. S. Guedes, D. D. Ferreira and B. H. G. Barbosa. "A non-intrusive approach to classify electrical appliances based on higher-order statistics and genetic algorithm: a smart grid perspective". *Electric Power Systems Research*, vol. 1, pp. 1–6, 2016. doi: 10.1016/j.epsr.2016.06.042.

[25] R. Naves, B. H. G. Barbosa and D. D. Ferreira. "Classification of Lung Sounds using Higher-Order Statistics: A divide-and-conquer approach". *Computer Methods and Programs in Biomedicine*, vol. 129, pp. 12–20, 2016. doi: 10.1016/j.cmpb.2016.02.013.

[26] K. Nazarpour, A. R. Sharafat and S. M. P. Firoozabadi. "Surface EMG signal classification using a selective mix of higher order statistics". In *Proceedings of the 27th Annual International Conference of the IEEE Engineering in Medicine and Biology Society*, pp. 4208–4211, 2005.

[27] K. Nazarpour, A. R. Sharafat and S. M. P. Firoozabadi. "Application of higher order statistics to surface electromyogram signal classification". *IEEE Transactions on Biomedical Engineering*, vol. 54, no. 10, pp. 1762–1769, 2007.

[28] E. Orosco, P. Diez, E. Laciar, V. Mut, C. Soria and F. di Sciascio. "On the use of high-order cumulant and bispectrum for muscular-activity detection". *Biomedical Signal Processing and Control*, vol. 18, pp. 325–333, 2015.

[29] C. Sapsanis, G. Georgoulas and A. Tzes. "EMG based classification of basic hand movements based on time-frequency features". In *21st Mediterranean Conference on Control & Automation (MED)*, pp. 716–722, 2013. doi: 10.1109/MED.2013.6608802.

[30] A. Phinyomark, F. Quaine, S. Charbonnier, C. Serviere, F. Tarpin-Bernard and Y. Laurillau. "EMG feature evaluation for improving myoelectric pattern recognition robustness". *Expert Systems with applications*, vol. 40, no. 12, pp. 4832–4840, 2013. doi: 10.1016/j.eswa.2013.02.023.

[31] K. Englehart and B. Hudgins. "A robust, real-time control scheme for multifunction myoelectric control". *IEEE transactions on biomedical engineering*, vol. 50, no. 7, pp. 848–854, 2003. doi: 10.1109/TBME.2003.813539.

[32] E. Scheme and K. Englehart. "Electromyogram pattern recognition for control of powered upper-limb prostheses: state of the art and challenges for clinical use". *Journal of Rehabilitation Research & Development*, vol. 48, no. 6, 2011. doi: 10.1682/JRRD.2010.09.0177.

[33] J. M. Mendel. "Tutorial on higher-order statistics (spectra) in signal processing and system theory: Theoretical results and some applications". *Proceedings of the IEEE*, vol. 79, no. 3, pp. 278–305, 1991. doi: 10.1109/5.75086.

[34] M. V. Ribeiro, C. A. G. Marques, C. A. Duque, A. S. Cerqueira and J. L. R. Pereira. "Detection of disturbances in voltage signals for power quality analysis using HOS". *EURASIP Journal on Advances in Signal Processing*, 2007. doi: 10.1155/2007/59786.

[35] H. Zhou, X. Wang and R. Zhu. "Feature selection based on mutual information with correlation coefficient". *Applied intelligence*, vol. 52, no. 5, pp. 5457–5474, 2022.

[36] R. J. Urbanowicz, M. Meeker, W. La Cava, R. S. Olson and J. H. Moore. "Relief-based feature selection: Introduction and review". *Journal of biomedical informatics*, vol. 85, pp. 189–203, 2018.

[37] I. Jo, S. Lee and S. Oh. "Improved measures of redundancy and relevance for mRMR feature selection". *Computers*, vol. 8, no. 2, pp. 42, 2019.

[38] M. B. Kursa, A. Jankowski and W. R. Rudnicki. "Boruta–a system for feature selection". *Fundamenta informaticae*, vol. 101, no. 4, pp. 271–285, 2010.

[39] F. Tahernezhad-Javazm, V. Azimirad and M. Shoaran. "A review and experimental study on the application of classifiers and evolutionary algorithms in EEG-based brain–machine interface systems". *Journal of neural engineering*, vol. 15, no. 2, pp. 021007, 2018. doi: 10.1088/1741-2552/aa8063.